CHEMISTRY
A EUROPEAN JOURNAL

DOI: 10.1002/chem.200500625

Ion-Triggered Multistate Molecular Switching Device Based on Regioselective Coordination-Controlled Ion Binding

Anne Petitjean,[a] Nathalie Kyritsakas,[b] and Jean-Marie Lehn*[a]

Abstract: Molecular devices capable of accessing different controlled conformational states, while optically signaling the occupied state, are attractive tools for nanotechnology since they relate to both areas of molecular mechanical devices and logic gates. We report here a simple molecular system that allows access to four distinct conformational and optical states. It is based on the regioselective complexation of metal ions to a heterocyclic ligand triad, which is dictated by the accessible coordination geometry and electrostatic properties of two distinct binding subunits. Thus, local conformational switching is brought about by tetrahedral coordination (of Cu^{I}) or octahedral coordination (of M^{2+} ions) to bidentate and tridentate binding subunits, respectively. The shape modifications undergone represent an ion-controlled nanomechanical device. They give controlled access to four different states that display different physicochemical (e.g. optical) properties and provide a basis for logic gate operations.

Keywords: conformational change · coordination modes · dynamic device · molecular switches · supramolecular chemistry

Introduction

Molecular devices capable of dynamic interconversion between different states are basic building blocks for nanotechnology. In particular, molecular switches[1] based on optical read-out (e.g., transmittance, luminescence) provide nanoscale signaling and information processing devices, while conformational switches open doors to the elaboration of nanoscale machines. In all cases, a simple, compact, and tractable molecule is desired, which integrates complex and addressable functions. On the other hand, systems accessing different states also play an important role in various *biological processes*, as illustrated by the molecular mechanism of vision.[2]

The design of molecular and supramolecular devices,[3,1a] allows in particular the elaboration of *molecular logic gates*[4] for nanotechnology. Much promise is to be found in the high complexity generated by increasing the number of states beyond two (0,1), which would lead to a higher density of information storage and hence assist both miniaturization and multiplexing. Among the potential modes of switching, photo- and electro-induced processes have received much attention.[5,6] Multistate switching may be difficult to implement in these systems as it requires performing the selective photo/electro-excitation of more than two units, and therefore designing multiple modules that have no excitation overlap (wavelength or potential). In this regard, switching through chemical triggers is more versatile. Although pH switching suffers from the same limitations as photo- and electro-induced switching (excitation of all sites of pK_a values higher than the imposed pH), this is not the case for ion-controlled switching. Indeed, the electronic information stored in organic ligands combined with the intrinsic properties of metal ions offers a wide range of affinities, providing a convenient handle on the selectivity, and, hence, on the complexity. As photo- and electro-induced switches are controlled by the intensity (power) and the excitation value (wavelength and voltage respectively) of the input stimulus, similarly ionic switches are operated on the basis of the concentration and the nature of the ions. Furthermore, the affinity of the ion may be modulated by additional factors such as oxidation state, hardness/softness of the binding site,[7] intrinsic coordination geometry preferences of the ion,[8] as well as accessible geometries of the considered ligand. Hence, each ion itself displays a range of ex-

[a] Dr. A. Petitjean, Prof. J.-M. Lehn
ISIS, Université Louis Pasteur
CNRS UMR 7006, BP 70028, 67083 Strasbourg (France)
Fax: (+33) 390-245-140
E-mail: lehn@isis.u-strasbg.fr

[b] N. Kyritsakas
Institut de Cristallochimie, Institut le Bel
Université Louis Pasteur
4 rue Blaise Pascal, 67000 Strasbourg (France)

WILEY InterScience DISCOVER SOMETHING GREAT
© 2005 Wiley-VCH Verlag GmbH & Co. KGaA, Weinheim

citation values, which adds further dimensions to the input modulation. As such, ionic switches offer a rare richness in accessible functional features.

We report here a molecular device that allows access to four distinct conformational and optical states. It is based on the regioselective coordination of two different metal ions to the heterocyclic triad LH, which is dictated by their selective binding to two suitably designed ligand subunits. Ion binding is accompanied by regioselective conformational modifications and by optical changes.

We have based our design on the control potential offered by the preference of metal ions for a given coordination geometry. Ligand LH (Scheme 1) was designed so as to offer a bidentate 2-pyridyl-4-pyrimidine (py–pym) motif as a privileged binding site with ions of tetrahedral coordination geometry, and a planar (O,N,N) tridentate unit including a 8-hydroxyquinoline group ($quin_{OH}$–pym), aimed at accommodating preferentially metal ions of octahedral coordination geometry. The latter was preferred over a terpyridine type subunit since it provides further tunability by means of its acido-basic activity. These bidentate and tridentate sites share a bridging pyrimidine unit expected to participate in both ion binding events. It was therefore anticipated that the bidentate binding site could be regioselectively switched by an ion such as copper(I), well-known to form tetracoordinate complexes with polypyridyl ligands (see below), whereas the terdentate subunit would preferentially bind a cation such as zinc(II) (Scheme 2). This binding selectivity may also be associated with soft/soft (py–pym site, Cu^{I}), hard/hard ($quin_{OH}$–pym, Zn^{II}) correspondence.

We have recently implemented in our group ligands containing two metal cation binding subunits based on terpyridine and bipyridine–pyrimidine groups, as ion-triggered nanomechanical switching devices[9,10] involving interconversion between two forms, of U and W shapes, of the ligand molecule. The present results incorporate regioselective control of ion binding and significantly extend the earlier work.

The corresponding events are schematically represented in Scheme 2. Furthermore, the overall process results in the regioselective self-assembly of a tetranuclear heterometallic-[2×2] grid architecture.[11]

Results and Discussion

Ligand LH: *Ligand synthesis*: A 2-substituted pyrimidine was chosen as the bridging unit in ligand LH, as the alkylphenyl substituent conveniently increases the solubility in organic solvents while also providing structural information (^{1}H NMR spectroscopy). To this end, 2-(4-*n*-butylphenyl)-4,6-dichloropyrimidine (**1**)[12] was successively coupled to a pyridinyl stannane and a quinolinyl stannane under Stille coupling conditions. 2-Tri-*n*-butylstannyl-6-methylpyridine[13] was quantitatively obtained from 2-bromo-6-methylpyridine[14] by *n*BuLi lithiation and reaction with tri-*n*-butyltin chloride followed by distillation. It was then coupled stoichiometrically with **1** to give **2** in moderate yields (Scheme 1). The quinoline fragment was prepared by oxidation of commercially available 8-hydroxyquinoline to the *N*-oxide derivative, rearrangement to the 2-oxo-1,2-dihydroquinolin-8-yl acetate **3** and bromination to the 2-bromo-quinolin-8-yl acetate **4**. The latter reaction proceeded in low yields due to simultaneous hydrolysis of the acetate. After stannylation of **4**, a Stille coupling was performed with the monochloropyrimidine **2** to yield the acetate-protected ligand **5**. Hydrolysis of the acetate proceeded smoothly in pyridine to yield the dissymmetric switch LH in sufficient amounts.

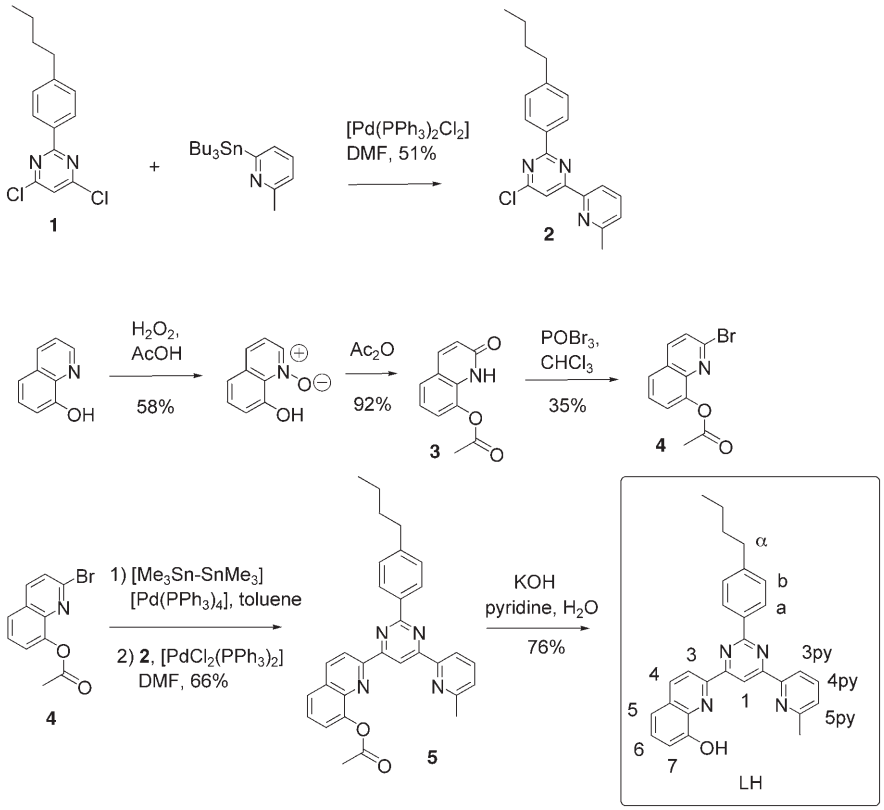

Scheme 1. Synthetic route to the heteroditopic ligand LH and proton numbering.

Ligand conformation: The ^{1}H NMR spectrum of ligand LH is characteristic of this type of U-shape molecule.[9] The preferred *transoid* conformation of 2,2′-bipyridine type

 © 2005 Wiley-VCH Verlag GmbH & Co. KGaA, Weinheim

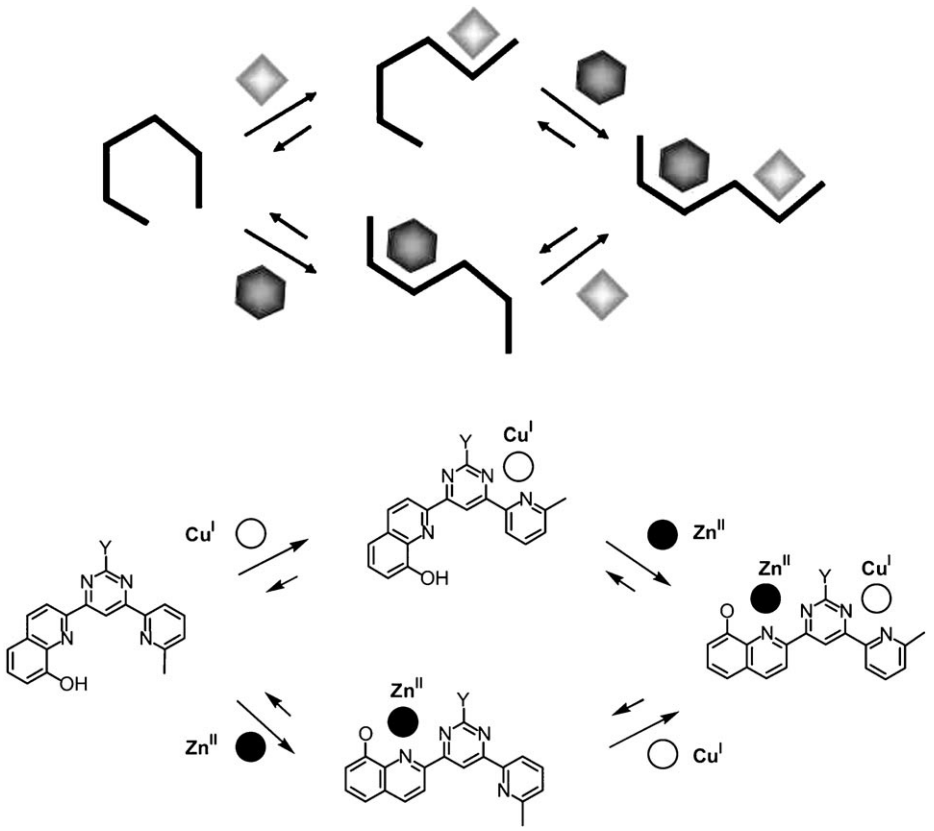

Scheme 2. Top: Schematic representation of the four-state structural switching of ligand LH operated by regioselective metal ion complexation; the bidentate and tridentate binding subunits in the ligand are represented by two and three segments respectively; squares and hexagons represent metal ions of tetrahedral and octahedral coordination geometry, respectively. Bottom: Structural representation of the ligand switching operated by regioselective, coordination algorithm-controlled binding of Cu^{I} and Zn^{II} cations.

diads[15] forces protons 1 and 3py (Scheme 1) to face the lone pair of the vicinal nitrogen atom, resulting in a strong downfield shift. Typically protons 1 and 3py give NMR signals at $\delta = 9.2$ and 8.5 ppm, respectively, as illustrated by the pyridine–pyrimidine–pyridine (py–pym–py) triad module.[9] The same deshielding effect holds for the quinolyl proton H3. The correlation between these high chemical shifts and the *transoid* conformation is confirmed by X-ray crystallography of similar compounds.[9,16] In the present case, the chemical shifts of protons 1, 3py, and 3 are indeed in agreement with an all *transoid* conformation for the 8-hydroxyquinoline–pyrimidine–pyridine ($quin_{OH}$–pym–py) triad in solution.

Regioselective switching performed by a metal ion of tetrahedral coordination : U-shaped py–pym–py triads having two identical bidentate binding sites have been reported previously to switch from a U to a W shape by a double conformational change upon the binding of two tetrahedrally coordinated copper(I) ions.[9] Similarly, progressive addition of copper(I) triflate to a solution of $quin_{OH}$–pym–py in $CDCl_3/CD_3CN$ induces a single conformational change that affects only the pym–py subunit of ligand LH, to give an S-shaped form, as illustrated in Scheme 2 and Figure 1. The proton NMR spectrum of the ligand undergoes marked changes in the course of the titration (Figure 1). Whereas the chemical shifts of the hydroxyquinoline protons remain constant ($\Delta\delta = \pm 0.05$ ppm), the signals of the protons 1, 3py, 4py, and 5py undergo significant shifts ($\Delta\delta = -0.2$, $+0.2$, and $+0.2$ ppm, respectively). The 2-pyrimidine aryl substituent protons (Ha and Hb) provide a sensitive probe for cation binding. Indeed, upon titration their signals are strongly shielded ($\delta = -0.5$ ppm), in accordance with the previously described U to W switching of the py–pym–py triad (validated by NOE analysis). Compared to the anthryl- and acridyl-substituted conformational switches reported previously,[9] the present ligand bears just a methyl group in position 6 of the pyridine unit, introduced to limit the susceptibility of Cu^{I} to oxidation. The lack of substantial steric hindrance in this position allows the stable 2:1, ligand–Cu^{I} complex to form.

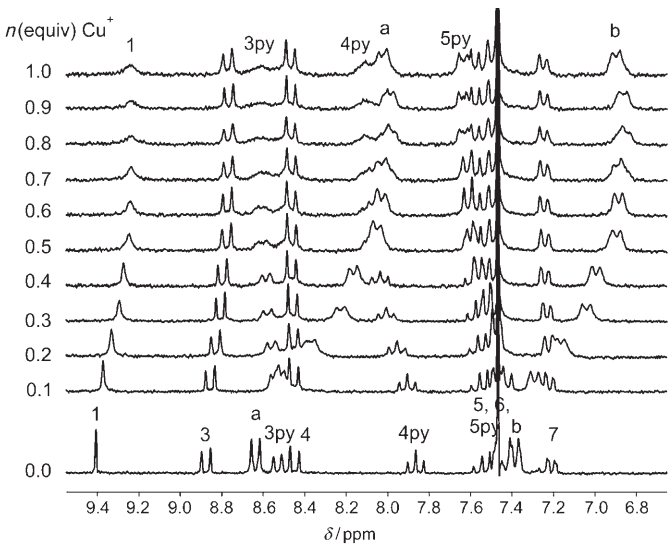

Figure 1. Aromatic region of the 200 MHz ^{1}H NMR spectrum of ligand LH (3.9 mM, 1:1 $CDCl_3/CD_3CN$) upon titration by a solution of $Cu^{I}(CH_3CN)_4BF_4$ (8 mM, same mixture of solvents). Proton numbering is given in Scheme 1.

© 2005 Wiley-VCH Verlag GmbH & Co. KGaA, Weinheim

The free ligand and the complex are in fast exchange on the NMR time scale, and analysis of the variation in chemical shifts upon copper titration[17a] (up to 1 equiv) is in agreement with the formation of the bis-bidentate species $[Cu^{I}(LH)_2]$ with a binding constant of intermediate strength: log β $[Cu^{I}(LH)_2]=7.6\pm0.6$ in 1:1 $CDCl_3/CD_3CN$. This value is higher than for the 1:1 complex between 6,6′-dimethyl-2,2′-bipyridine and Cu^{I} in pure acetonitrile (log $\beta=6.1\pm0.1$).[17b] The corresponding bis-bidentate 2:1 complex is about five orders of magnitude stronger (log $\beta=11.6\pm0.05$)[17c] and presents a tetrahedral coordination geometry.[18] As the 2:1 complex is much more stable than the 1:1 species, only the former is detected in the range of Cu^{I} concentrations used here. The dimerization also correlates with the large NMR shielding shifts experienced by the protons on the pym substituents (Ha, Hb, and Hα) and takes place by formation of a tetrahedral Cu^{I} coordination site.[18] Electrospray mass spectrometry measurements show the coexistence of both $[CuLH]^+$ and $[Cu(LH)_2]^+$ complexes in the gas phase. The lower binding constant compared to the parent $[Cu^{I}(2,2'\text{-bipyridine})_2]$ complex may result from a combination of the less basic N coordination site of the pyrimidine group in the pym–py diad compared to a pyridine N site, and the steric constraints due to the aryl substituent on the pym unit. In the ligands of the previously reported switching devices,[9] the anthryl and acridinyl pyridyl substituents and the phenyl pyrimidyl substituent prohibit the formation of the 2:1 complex, resulting in a weak coordination of Cu^{I} in a 1:1 stoichiometry (log $\beta=2.93\pm0.07$). Independent of the exact stoichiometry of the complex, the ^{1}H NMR titration spectra shown in Figure 1 clearly testify that the present dissymmetric ligand LH is regioselectively switched to the *cisoid* form on the pym–py side by a tetrahedrally coordinating "soft" cation such as Cu^{I}, as anticipated from previous work.[9]

Regioselective switching performed by a metal ion of octahedral coordination: In contrast to the pym–py coordination subunit already used previously,[9] the $quin_{OH}$–pym motif is a novel triad for switchable devices. In addition to the advantage of being tridentate and, hence, a strong binder, the presence of a hydroxy group provides an anchoring site for oxophilic and "hard" cations. Furthermore, its ionizable hydroxy group provides pH tunability of this binding site (see below).

To enhance the differentiation of the two pym–py and $quin_{OH}$–pym coordination modules, the introduction of a divalent cation was coupled to ionization of the hydroxy site to $quin_O$–pym by addition of one equivalent of Me_4NOH to generate the phenoxide ligand L^-.

Conformational change induced by Zn^{II} ions: Zinc(II) is an appropriate cation for coordination to the $quin_O$–pym subunit: being oxophilic, it should help targeting the oxygen-containing binding site while keeping a reasonable affinity for nitrogen-containing ligands. Addition of zinc(II) triflate to a solution of L^- shows two regimes with increasing $[Zn]^{2+}$:

- Up to 0.5 equivalents of Zn^{2+}, a new complex is formed, characterized by a lower chemical shift of H1 ($\delta_{H1}=8.30$ ppm), consistent with switching to a *cisoid* conformation. ^{1}H NMR ROESY experiments show that protons H1 and H3 are indeed close to each other, whereas no correlation was observed between H1 and H3py, which confirms the regioselective conformational change on the $quin_O$–pym terdentate binding site. The strong shielding of protons Ha and Hb, as in the titration with Cu^{I}, suggests the formation of a dimeric complex, in agreement with the FAB mass spectrum where the 2:1 complex is exclusively identified. X-ray crystallography confirms the assignment of this first species as the neutral ZnL_2 complex, in which the $quin_O$–pym subunit of the two ligands is regioselectively switched (Figure 2). In

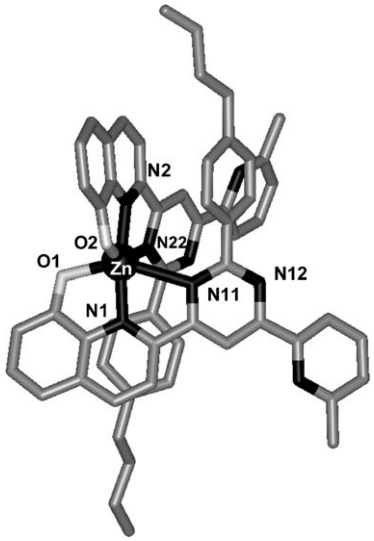

Figure 2. Solid-state molecular structure of the dimeric ZnL_2 complex (hydrogen atoms and solvent molecules are omitted for clarity).

the solid state, the zinc cation is strongly bound by the hydroxyquinoline anion (Zn–O1 2.078, Zn–O2 2.066, Zn–N1 2.032, Zn–N2 2.036 Å). The interactions between the zinc cation and the pyrimidine nitrogen atoms N11 and N22 are much weaker with larger interatomic distances (Zn–N11 2.51 and Zn–N22 2.55 Å), as anticipated in view of the lower basicity of these sites. This weaker interaction allows additional stabilization elements to be expressed, such as a weak hydrogen bond between the pyrimidine nitrogen sites and the vicinal aryl proton (Ha–N12 2.63 Å) and π-stacking interactions between the quinoline and the alkylaryl moieties (plane-to-plane distance: 3.4 Å).

- Increasing the amount of Zn^{2+} above 0.5 equivalents results in the formation of a second complex, in slow exchange with ZnL_2, in which the chemical shift of H1 is still lower ($\delta_{H1}=7.97$ ppm; spectrum not shown). The existence of a cross-peak between H1 and H3py (as well as one for H1 and H3) suggests that this new complex also involves the pym–py binding subunit. ES mass spectrom-

 © 2005 Wiley-VCH Verlag GmbH & Co. KGaA, Weinheim

etry confirms the formation of multinuclear complexes of the type $Zn_3L_3^{2+}$ and $Zn_2L_3^{+}$. The involvement of the pym–py binding site as a stoichiometric amount of Zn^{2+} is reached is not surprising, as the latter is a better ligand than the solvent molecules (CD_3CN or CD_3OD).

To perform a regioselective switch of the $quin_O$–pym with a 1/1 stoichiometric amount of Zn^{2+}, a capping ligand may be introduced prior to titration. 2,6-Bis(*N*,*N*-dimethylhydrazonomethyl)pyridine (DMHP, Figure 3) was chosen as an

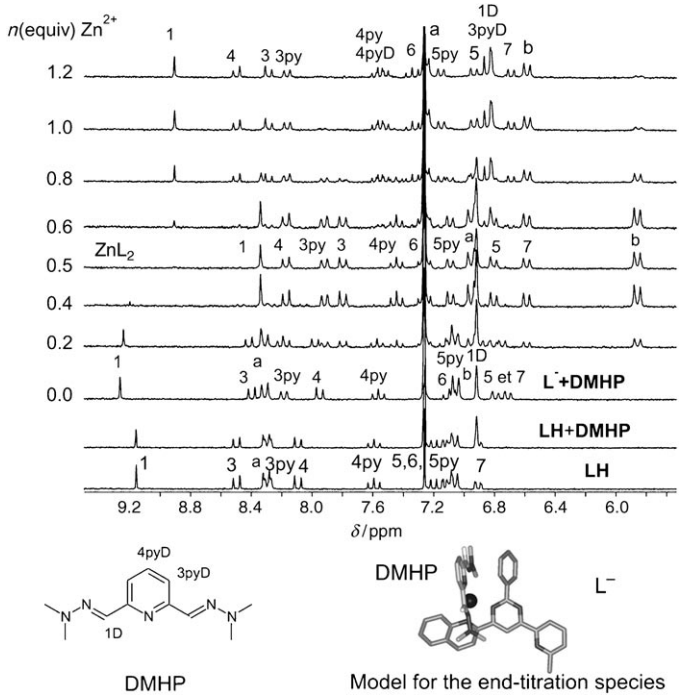

Figure 3. Aromatic region of the 200 MHz ^{1}H NMR spectrum of the 1:1 mixture of ligand L^- and DMHP (3.5 mM in 1:1 $CDCl_3/CD_3OD$) upon titration by a solution of $Zn^{II}(TfO)_2$ (8.9 mM, same mixture of solvents). Proton numbering is detailed in Scheme 1. A model of the final complex is represented on the bottom right (the alkyl substituent is omitted).

additional terdentate ligand, analogous to terpyridine but yielding fewer NMR signals. The ^{1}H NMR spectra for the titration of a mixture of L^- and DMHP by Zn^{2+} are shown in Figure 3. Up to 0.5 equivalents, L^- forms the same neutral quinoline-bound complex ZnL_2 as in the absence of DMHP. The DMHP signals are not affected by the initial introduction of zinc(II) ions, although the pyridine and hydrazone binding sites themselves are expected to be strong enough to override the weak pyrimidine nitrogen atom, showing the importance of electrostatic interactions $-O^-,Zn^{2+}$ in this system. Above 0.5 equivalents, DMHP is involved in a slow exchange with a new compound; the chemical shift of its proton signal in position 4 of the pyridine group increases (as expected for a coordinated pyridine) and the protons 3pyD and 1D (Figure 3) are shielded, as anticipated for a change from a *transoid* to a *cisoid* conformation. As for the ligand, the intermediate chemical shift for H1 between that of the free ionized ligand L^- ($\delta = 9.25$ ppm) and that of the dimeric ZnL_2 complex ($\delta = 8.30$ ppm) is in agreement with a regioselective switch. One notes also that the pyridyl chemical shifts of the pym–py module (3py, 4py, and 5py), slightly affected by the dimerization to ZnL_2, are restored to their initial in L^- values. ROESY experiments confirm the regioselective conformational change of the $quin_O$–pym binding subunit, showing cross-peaks between H1 and H3, consistent with a *cisoid* conformation of the $quin_O$–pym unit, but not between H1 and H3py. In addition, the conserved *transoid* conformation of the py–pym fragment is confirmed by a weak correlation between the pyridyl H3py and the aryl Ha protons. The incorporation of the DMHP ligand into the complex is supported by NOE cross-peaks between the methyl groups of the DMHP moiety and the pyrimidine H1 proton on one hand, and the aryl Ha protons on the other; both interactions can be accounted for if the DMHP ligand is free to rock across the L^- ligand (see model in Figure 3).

Conformational change induced by Pb^{II} ions: Lead(II) ions were also considered as potential triggers for the regioselective switching of the terdentate binding site. With an ionic radius about 1.5 times that of zinc(II), lead(II) is a "softer" cation. Still, it binds to the $quin_O$–pym unit of L^- as indicated by the ^{1}H NMR data (not shown). In addition to the unchanged chemical shifts of the pyridyl protons, the absence of cross-peaks between H1 and H3py, complemented by the proximity of Ha and H3py, support a *transoid* conformation of the pym–py module. On the other hand, the $quin_O$–pym unit adopts a *cisoid* conformation, as shown by the NOE cross-peak between H1 and H3. The examination of the aliphatic region of the spectrum suggests the interaction of two ligands within the same complex, but not in a 2:1 ligand-to-metal ratio, as it takes one equivalent to reach a well defined spectrum, and the NOE cross-peaks between the first aliphatic protons (Hα) and the H6 quinoline protons (see Figure 4) cannot be explained by a ZnL_2-type complex. The occurrence of dimerization was confirmed by a single-crystal X-ray diffraction study of the complex, which showed the formation of a dimeric species indeed incorporating two ligands and two lead ions bridged through the oxide groups (Figure 4). The solid-state structure clearly displays the binding of the $quin_O$–pym unit with a strong contribution from the quinoline heterocycle (Pb1–O1 2.275 Å, Pb1–N1 2.496 Å), and a weak contribution of the pyrimidine-nitrogen atom (Pb1–N11 2.780 Å). The two lead ions are unsymmetrically bound to the two bridging oxide sites (Pb1–O2 2.554 Å) and two counteranions provide additional unsymmetrical axial bridges (Pb1–O3 2.455, Pb2–O4 2.722 Å). Overall, the lead cations adopt a distorted octahedral coordination mode with two ligands L^- essentially in the same plane and triflate anions as axial ligands. This situation confers an interesting long-range organization to the crystal, consisting of intertwined tubular ionic channels in which the cationic dimers are relayed by triflate anions, which themselves form hydrogen bonds to the H4py protons of peripheral channels. Overall, the stacked organic ligands define a

 © 2005 Wiley-VCH Verlag GmbH & Co. KGaA, Weinheim

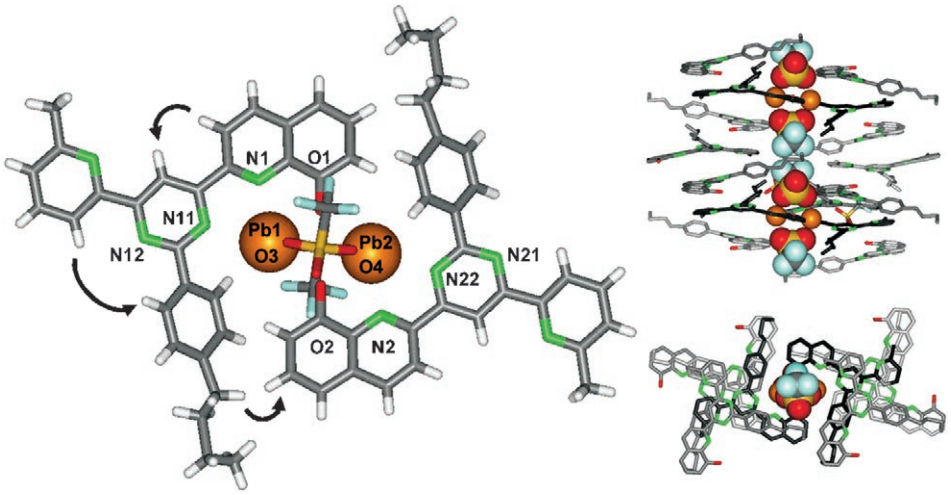

Figure 4. Solid-state molecular structure of the dimeric $Pb_2L_2(TfO^-)_2$ complex; left: dimer alone (the black arrows represent NOEs observed in solution); right: side (top) and top (bottom) views of the ion-containing channels formed in the crystal (hydrogen atoms, solvent molecules and noncoordinative counteranions are omitted for clarity). Different levels of gray are used for the different layers of ligands. Pb^{2+} and coordinated triflate ions are represented as CPK models.

four-fold symmetric intertwined channel system (Figure 4, right).

The ^{1}H NMR and crystallographic studies therefore confirm the regioselective switching process from the *transoid* to the *cisoid* form performed by divalent metal cations on the $quin_O$–pym subunit of ligand L^-.

pH modulation of the binding properties of the terdentate $quin_{OH}$–pym subunit: A*n acido-basic switch for trivalent lanthanide cations*: In the case of zinc, ionization of ligand LH was necessary to obtain well-defined complexes, suggesting that this borderline ion has sufficient affinity for nitrogen sites to bind to both $quin_O$–pym and py–pym modules in the neutral state. It was therefore interesting to investigate cations that would not bind the ligand in its neutral state, and become good substrates upon basification, to perform pH-induced conformational switching. Harder labile cations were therefore required, in particular trivalent lanthanide ions such as lanthanum(III), which offered the possibility to conveniently monitor the conformational change by ^{1}H NMR spectroscopy. As illustrated in Figure 5, addition of Ln^{3+} to LH does not yield any significant change in the chemical shifts of the ligand. Addition of one equivalent of tetramethylammonium hydroxide to the solution cleanly gives rise to a single complex whose spectrum resembles that of ZnL_2 ($\delta_{H1}=8.41$ ppm). ES-MS is consistent with the dimeric nature of this complex, LaL_2^+ being the only observed species. ROESY NMR experiments confirm the conformational change of the $quin_O$–pym unit exclusively, as H1 is in close contact with H3 but not with H3py. Addition of one equivalent of TFA to the complex protonates the ligand and releases the lanthanum cation, as evidenced by the restored chemical shifts of ligand LH (Figure 5). The protonation/deprotonation cycle can be consistently performed several times, as illustrated in Figure 5.

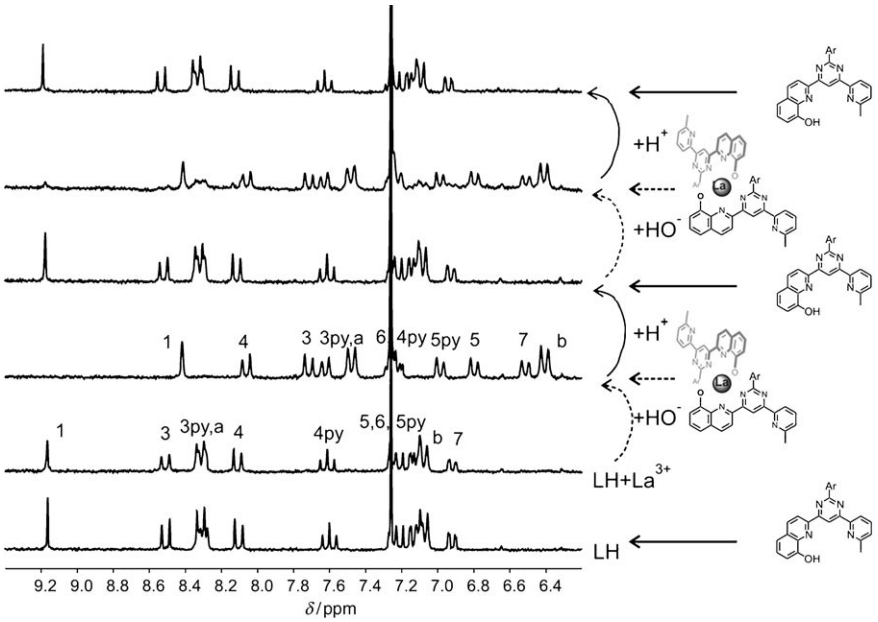

Figure 5. Aromatic region of the 200 MHz ^{1}H NMR spectrum of LH (L^-) in the presence of La^{3+} (4 mM, 1:1 $CDCl_3/CD_3OD$), and reversible pH modulation of its binding affinity.

Dual regioselective switching and ion-selective self-assembly of [2×2] heterometallic grid complexes: The free ligand, the copper(I) py–pym-bound complex, and the zinc(II) $quin_O$–pym chelate provide three different ligand conformational states. Since copper(I) and zinc(II) can be incorporated independently, we studied the access to a fourth state in which both binding modules would be in a *cisoid* complexed form. The proton NMR spectral changes occurring on addition of copper(I) to the $[Zn^{II}(L^-)(DMHP)]^+$ complex are displayed in Figure 6, and show the formation of a new species in slow exchange with the starting complex. This observation com-

 © 2005 Wiley-VCH Verlag GmbH & Co. KGaA, Weinheim

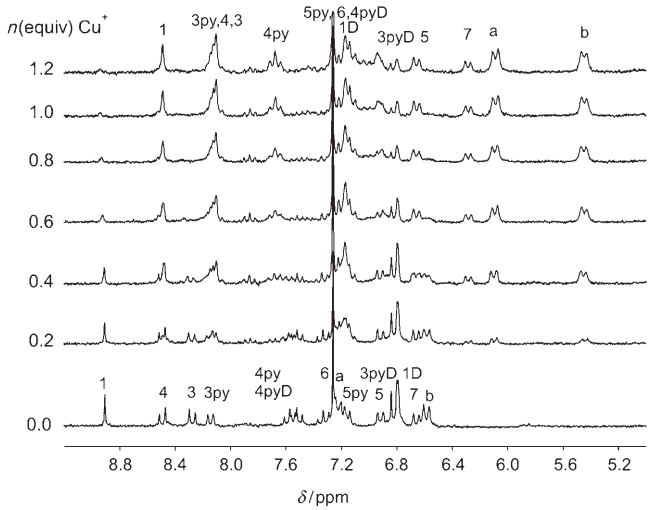

Figure 6. 200 MHz ^{1}H NMR spectra for the titration of $[Zn^{II}(L^-)(DMHP)]^+$ by $Cu^I(CH_3CN)_4^+$ in 2:1:1 $CDCl_3/CD_3CN/CD_3OD$ (aromatic region).

bined with the deep violet color and the very shielded signal for Ha and Hb protons suggests a more complex architecture than the anticipated $[Zn^{II}Cu^I(L)(DMHP)]^{2+}$ complex. ES-MS analysis of the titration end-point reveals that the DMHP ligand is expelled from the complex and picks up Cu^+ and Zn^{2+} ions ($[Cu^I(DMHP)_2]^+$ and $[Zn^{II}(DMHP)_2]^{2+}$ detected), whereas four L-type ligands assemble with two copper(I) ions and two zinc(II) ions giving ES-MS signals for the complexes: $[(Zn^{II})_2(Cu^I)_2(L^-)_2(LH)_2]^{4+}$; $[(Zn^{II})_2(Cu^I)_2(L^-)_2(LH)_2]^{4+}$, TfO^-, and $[(Zn^{II})_2(Cu^I)_2(L^-)_4]^{2+}$. A species with identical NMR signature is indeed obtained on directly mixing L^- with Cu^I and Zn^{II} in a 4:2:2 ratio. It was characterized by ^{1}H NMR spectroscopy and by X-ray crystallography (Figure 7), confirming the formation of a [2×2] grid-like structure, with combined conformational change of both coordination modules.[11,19]

Interestingly, Cu^{II} may be used instead of Zn^{II}. Although ^{1}H NMR spectroscopy could not serve to monitor the conformational change because of the paramagnetic properties

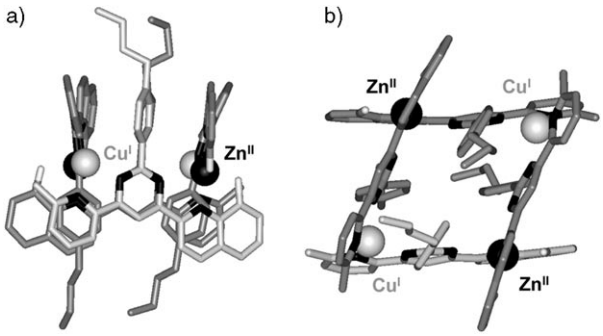

Figure 7. Two views of the solid state molecular structure of complex $[Zn_2Cu_2L_4]^{2+}$ $(TfO^-)_2$ (hydrogen atoms, solvent molecules and counteranions are omitted for clarity; the front ligand is represented in light gray for clarity); see also reference [10].

of Cu^{II}, the color of the 4 L,2Cu^I,2Cu^{II} solution (see below) and the mass spectrometry studies suggest the formation of the analogous $[(Cu^{II})_2(Cu^I)_2(L^-)_4]^{2+}$ complex. The observation that a single cation in two different interconvertible oxidation states may be used to operate the conformational switch suggests exciting extensions towards electro-controlled ionic conformational switches.

These processes amount to the regioselective self-assembly of a heterometallic tetranuclear [2×2] grid-type architecture, directed by the reading out of the ion-binding information of ligand L^- by tetrahedral and octahedral coordination algorithms.[20] They represent the programmed introduction in a single operation of different ions (ion selectivity) at precisely defined locations (toposelectivity) in a polymetallic supramolecular architecture, an ultimate goal of self-organization of metallosupramolecular architectures.

Multistate ionic switching devices as the basis for complex logic gates: Four different states can be accessed by the present system depending on the species in presence, each of them being characterized by different electronic absorption features. LH and its ionized form having their highest absorption peak at 326 nm are colorless. Addition of Cu^+ to LH introduces an absorption band in the visible region (391 nm) responsible for the pale orange color of the complex. A red color, greatly enhanced in basic media, is activated by complexation of either Cu^{2+}, Zn^{2+}, Pb^{2+}, or La^{3+} (broad band centered around 480 nm). Finally, the combination of both monovalent and multivalent ions provides a fourth state absorbing at the highest wavelength (broad band centered around 555 nm) and is responsible for a deep purple color (Figure 8).

Marked interest has been shown recently in the design of molecular and supramolecular devices presenting logic gate features.[4,21] The processes undergone by the present system may also be analyzed along such lines. Indeed, modulation of the number of the input triggers generating the four optical output values gives access to a complex set of logic states, as detailed in Table 1, Table 2, and Table 3.

LH operates as an AND logic gate by activating the absorption around 480 nm when *both* HO^- and multivalent cations (Zn^{2+}, Pb^{2+}, Cu^{2+}, or La^{3+}) are present (Table 1). Either of the above-mentioned multivalent ions can be used, therefore combining the AND function with an OR operation. The latter tolerates any multiply charged species since it is based on the charge-controlled binding of the metal ion, to the ionized phenoxo site. Therefore all divalent (Cu^{2+}, Pb^{2+}, Zn^{2+}) and trivalent (La^{3+}) cations are possible operators. The binding is nevertheless conditioned by the ionization of the phenoxide function responsible for the appropriate hardness of the ligand, imposing an AND function (Table 1).

In the case of the triply charged La^{3+} cation, there is no interaction at all with neutral LH and deprotonation is necessary for binding and any detectable coloring to occur. This translates into a proton-induced INHIBIT operation at 480 nm, as expressed in Table 2.

 © 2005 Wiley-VCH Verlag GmbH & Co. KGaA, Weinheim

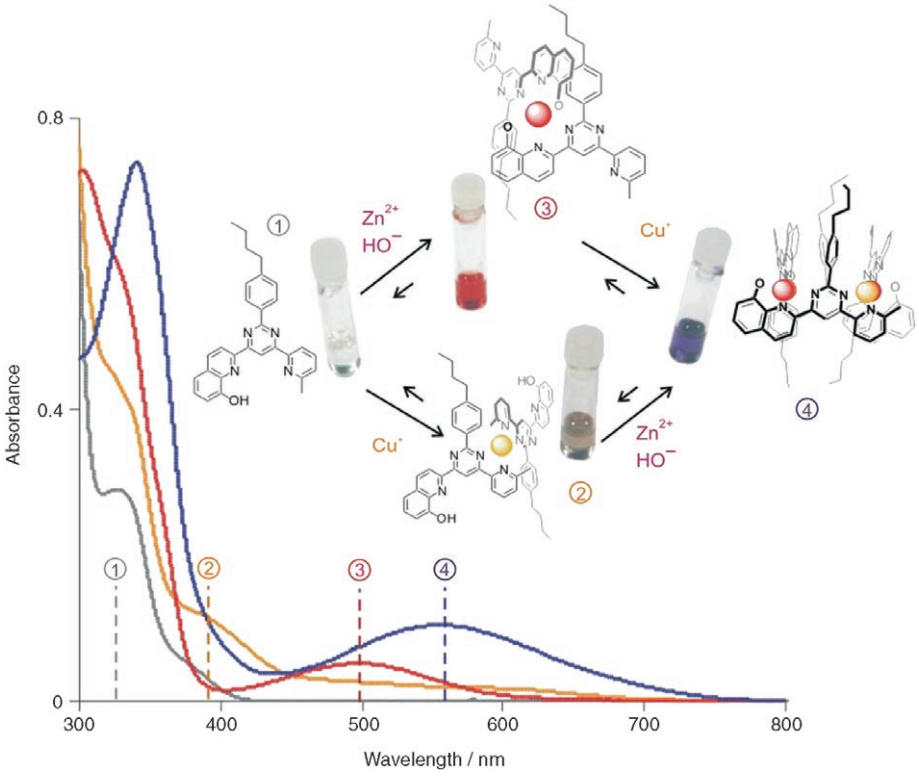

Figure 8. The system LH/metal ion/HO^- as a iono-mechanical double switching device operated by several different inputs and generating four different outputs.

pale yellow complexes absorb in distinct visible regions (390 nm and 480 nm) and act as individual distinct outputs. On the other hand, the purple species is characterized by broad bands covering all four wavelengths significantly, and, hence, activating several outputs simultaneously.

Conclusion

As demonstrated above, molecule LH is able to access four conformational states depending on its interaction with different ions such as Cu^I, Zn^{II}, Ln^{III}, and H^+/HO^-. The capacity to specifically address particular sites (e.g., H^+/HO^- affect the hydroxy group, Cu^I and Zn^{II} target the py–pym and $quin_O$–pym modules respectively) and the possibility to activate all stimuli simultaneously are highly valuable assets of ionically operated processes compared to the photonic and electronic modes. Furthermore, the ability of cations to modulate the electronic properties of their ligand (not to mention the intrinsic electronic richness of d transition metal cations) confers an additional interest to ionic switches. In the present case, the four different conformational states are associated with four distinct optical states, namely the colorless LH and L^- ligands ($\lambda_{max}=326$ nm), the py–pym switched light orange $[Cu(LH)_2]$ complex ($\lambda_{max}=390$ nm), the $quin_O$–pym bound bright red $[Zn(L)_2]$, $[Zn(L^-)(DMHP)]^+$, and $[Ln(L^-)_2]^+$ complexes ($\lambda_{max}=480$ nm), and the doubly switched deep purple $[(Zn^{II})_2(Cu^I)_2(L^-)_4]^{2+}$ grid ($\lambda_{max}=555$ nm). This system thus represents an opto-ionic molecular switching device[3,22] involving multiple chemical/ionic inputs and multiple optical outputs,

Table 1. M^{n+} AND HO^- logic gate (M^{n+}: Zn^{2+}, Cu^{2+}, Pb^{2+}, La^{3+}).

Input 1 M^{n+}	Input 2 HO^-	Output 3 480 nm
0	0	0
0	1	0
0	1	0
1	0	0
1	1	1

Table 2. INHIBIT logic gate

Input 1 La^{3+}	Input 2 HO^-	Input 3 H^+	Output 3 480 nm
0	0	0	0
1	0	0	0
0	1	0	0
0	0	1	0
1	1	0	1
1	0	1	0
0	1	1	0
1	1	1	0

In addition to integrating several operation modes depending on the read output (and therefore on different input triggers), the present unit LH operates via two switching components based on conformational changes, thus enabling the activation of several output values simultaneously or independently (Table 3). On the one hand, the red and

Table 3. Multiple input/multiple output logic gate (M^{n+} are multivalent ions such as Cu^{2+}, Pb^{2+}, Zn^{2+}, and La^{3+}). The state of the switch relates to the *anti* (OFF) and *syn* (ON) conformations of the py–pym and $quin_O$–pym components, where *syn* is the form induced by cation binding.

Input	Switch component state			Outputs			
				λ_{max} [nm]			
2 Cu^+	3 and 4 M^{n+} and HO^-	py–pym	$quin_O$–pym	1 326	2 390	3 480	4 555
0	0	OFF	OFF	1	0	0	0
1	0	ON	OFF	1	1	0	0
0	1	OFF	ON	1	0	1	0
1	1	ON	ON	1	1	1	1

 © 2005 Wiley-VCH Verlag GmbH & Co. KGaA, Weinheim

and effecting the generation and conversion of chemicals signals, features of much interest for the development of semiochemistry.[3] The combined controlled mechanical motions, the selective optical read-out and the addressing of several distinct states demonstrate the potential of reversible, ionically operated, multistate molecular switching devices in accessing nanoscale entities presenting functional features of interest for the design and operation of molecular computational and signaling processes of increased complexity.

Experimental Section

^{1}H and ^{13}C NMR spectra were recorded on a Bruker AC 200 (200 MHz and 50 MHz respectively) at 25 °C. ^{1}H NMR titrations were conducted on a Bruker AC 200 spectrometer at 25 °C. $CDCl_3$ was freshly neutralized by passing through dried basic alumina prior to each experiment; all NMR solvents were degassed by bubbling argon prior to titration. For ^{1}H NMR titrations, determined volumes of a solution of the titrant (triflate or tetrafluoroborate salt solution) of known concentration (typically 10–25 mM) in a solvent or mixture of solvents were added to a solution of the receptor (typically 2–5 mM) in the same mixture of solvent, and the chemical shift of all protons monitored. Mass spectrometry was performed in the Laboratoire de Spectrométrie de masse Bio-organique (Strasbourg) and elemental analyses at the elemental analysis service of Louis Pasteur University (Strasbourg). UV/Vis spectra were recorded on a Shimadzu HYPER UV using 110-QS Hellma Cuve quartz (10 mm and 0.1 mm) and degassed solvents. As in the case of the NMR measurements, $CHCl_3$ was neutralized by passing through dried basic alumina prior to preparing the stock solutions. All reagents were used as received. Dry solvents (dichloromethane, toluene, THF) were distilled over drying agents (calcium hydride, Na, Na/benzophenone, respectively) under argon. DMHP was obtained by condensation of dimethylhydrazine with commercially available 2,6-pyridinedicarboxaldehyde (Aldrich).[23] Crystal data were collected at 173 K on a Nonius KappaCCD diffractometer, and structures were solved by Nathalie Kyristakas at the Service Commun de Cristallographie (Louis Pasteur University, Strasbourg) using (Bruker) SAINT and SHELXTL 97 software.

Crystallographic data: Single crystals of the complex ZnL_2 ($[2C_{58}H_{50}N_8O_2Zn]\cdot 3CH_3OH$) were grown by slow diffusion of diethyl ether into a mM solution (mixture of $CDCl_3$ and CD_3OD). Crystals were placed in oil and a single dark red crystal of dimensions $0.10\times0.10\times0.08$ mm mounted on a glass fiber and placed in a low-temperature N_2 stream. The cell was triclinic; space group $P\bar{1}$. Cell dimensions: $a=11.5751$, $b=15.7037$, $c=15.7449$ Å, $\alpha=\gamma=67.384°$, $\beta=77.212°$, $\gamma=70.964°$, $V=2482.3$, and $Z=1$ (FW = 2009.06 and $\rho=1.34\,g\,cm^{-1-3}$). A total of 14458 reflections were collected ($2.5°\leq\theta\leq30.06°$), of which 10530 were unique, having $I>3\sigma(I)$; 648 parameters. Final R factors were $R_1=0.049$ (based on observed data) and $wR_2=0.342$ (based on all data), GOF = 1.457, maximal residual electron density is 0.880 e Å^{-3}.

Single crystals of the complex Pb_2L_2 ($[C_{29}H_{25}N_4OPb]\cdot F_3CSO_3$) spontaneously formed from a 2 mM solution of the complex in 1:1 $CDCl_3/CD_3CN$. Crystals were placed in oil and a single yellow prism of dimensions $0.16\times0.14\times0.12$ mm mounted on a glass fiber and placed in a low-temperature N_2 stream. The cell was tetragonal; space group of $I41/a$. Cell dimensions: $a=b=29.9186$, $c=13.0566$ Å, $V=11687.3$ and Z = 16 (FW = 801.81 and $\rho=1.82\,g\,cm^{-3}$). A total of 8888 reflections were collected ($2.5°\leq\theta\leq30.06°$), of which 5396 were unique, having $I>3\sigma(I)$; 356 parameters. Final R factors were $R_1=0.048$ (based on observed data) and $wR_2=0.078$ (based on all data), GOF = 1.433, maximal residual electron density is 0.924 e Å^{-3}.

CCDC-271555 (Pb_2L_2) and CCDC-271556 (ZnL_2) contain the supplementary crystallographic data for this paper. These data can be obtained free of charge from The Cambridge Crystallographic Data Centre via www.ccdc.cam.ac.uk/data_request/cif.

2-Tri-*n*-butylstannyl-6-methylpyridine:[13] *n*-Butyllithium (17 mL; 1.6 M in hexane (27 mmol, 1.15 equiv)) was added dropwise to 2-bromo-6-methylpyridine[14] (4.00 g, 23.3 mmol) solubilized in dry THF (30 mL) and cooled down to −78 °C under argon. After the mixture had been stirred for 1 h at −78 °C, tri-*n*-butyltin chloride (8.0 mL, 29 mmol, 1.3 equiv) was added dropwise to the red solution. The orange solution was then stirred overnight. After evaporation of the solvent, the residue was taken up in diethyl ether (50 mL) and water (20 mL). The organic layer was further washed with brine (15 mL) and the combined aqueous layers extracted with diethyl ether (2×15 mL). The combined organic layers were dried (Na_2SO_4), filtered, and concentrated in vacuo. Distillation of the crude product (115–120 °C at 0.1 mmHg) afforded the desired stannane (8.8 g; 99 % yield). ^{1}H NMR ($CDCl_3$): $\delta=7.36$ (t, $^3J=7.3$ Hz, 1H), 7.17 (d, $^3J=8$ Hz, 1H), 6.95 (dd, $^3J=7.7$ Hz, $^4J=0.9$ Hz, 1H), 2.54 (s, 3H), 0.8–1.7 ppm (m, 16H).

2-(4-*n*-Butylphenyl)-4-chloro-6-(6-methylpyridin-2-yl)-pyrimidine (2): 2-Tri-*n*-butylstannyl-6-methylpyridine (4.05 g, 10.6 mmol), 2-(4-*n*-butylphenyl)-4,6-dichloropyrimidine[12] (3.06 g, 10.9 mmol, 1.05 equiv), and dichlorobistriphenylphosphinepalladium(II) (155 mg, 2.2×10^{-4} mol, 0.02 equiv) were mixed in degassed DMF under argon and heated at 80 °C for 36 h. After removal of the solvent, the solid residue was dissolved in diethyl ether (70 mL) and washed with an aqueous solution of potassium fluoride (9 g in 90 mL). The aqueous layer was extracted with diethyl ether (30 mL) and dried (Na_2SO_4), filtered, and concentrated. After purification by column chromatography (flash, SiO_2, hexane/CH_2Cl_2 50:5 to 50:10), a shiny white solid was obtained (1.84 g, 51 %). ^{1}H NMR ($CDCl_3$) : $\delta=8.4$–8.5 (m, 3H), 8.29 (s, 1H), 7.78 (t, $^3J=7.7$ Hz, 1H), 7.2–7.4 (m, 3H), 2.70 (t, $^3J=7.4$ Hz), 2.66 (s, 3H, CH_3), 1,66 (quint., $^3J=7.8$ Hz), 1.39 (sext., $^3J=7.8$ Hz, 2H), 0.95 ppm (t, $^3J=7.4$ Hz, 3H); ^{13}C NMR ($CDCl_3$): $\delta=165.1$, 164.8, 162.6, 158.5, 152.7, 146.7, 137.2, 134.0, 128.7, 128.6, 125.4; 119.3, 115.0, 35.7, 33.4, 24.6, 22.4, 14.0 ppm: R_f (SiO_2, hexane/CH_2Cl_2 5:1) = 0.28; m.p. 89 °C. EI: 337.3 ($[M]^-$); elemental analysis calcd (%) for $C_{20}H_{20}N_3Cl\cdot0.15\,CH_2Cl_2$: C 70.89, H 5.95, N 12.35, Cl 10.45; found: C 70.88, H 5.99, N 12.61.

8-Hydroxyquinoline-*N*-oxide:[24] Hydrogen peroxide (8 mL, 30–35 % in water) was added dropwise to a solution of commercially available 8-hydroxyquinoline (3.00 g, 20.7 mmol) in acetic acid (35 mL); the solution was then refluxed for 40 min. After solvent removal, the oily residue was taken up in dichloromethane (50 mL) and washed with a dilute aqueous solution of hydrogen carbonate (pH 6–7). The aqueous layer was extracted with dichloromethane (3×30 mL) and the combined organic layers were dried (Na_2SO_4), filtered, and concentrated in vacuo before column chromatography (SiO_2, CH_2Cl_2/acetone 2.0:0.2 to 2.0:0.4) to afford a yellow solid (3.85 g; 58 %). ^{1}H NMR ($CDCl_3$): $\delta=8.23$ (d, $^3J=6.0$ Hz, 1H), 7.78 (d, $^3J=8.4$ Hz, 1H), 7.49 (t, $^3J=8.0$ Hz, 1H), 7.15–7.25 (m, 2H), 7.06 ppm (dd, $^3J=7.9$ Hz, $^4J=0.9$ Hz, 1H).

2-Oxo-1,2-dihydroquinolin-8-yl acetate (3):[25] A suspension of 8-hydroxyquinoline-*N*-oxide (2.00 g, 12.4 mmol) in acetic anhydride (12 mL) was heated to 100 °C for 7.5 h under an atmosphere of dinitrogen. The beige solid was poured into water (50 mL), cooled in an ice bath, and neutralized with a concentrated aqueous ammonia solution. The solid was filtered, washed with water, and dried in vacuo, to afford a beige solid (2.32 g; 92 %). ^{1}H NMR ($CDCl_3$): $\delta=10.8$ (br s, 1H), 7.77 (d, $^3J=9.6$ Hz, 1H), 7.43 (dd, $^3J=7.7$ Hz, $^4J=1.3$ Hz, 1H), 7.36 (dd, $^3J=8.0$ Hz, $^4J=1.3$ Hz, 1H), 7.19 (t, $^3J=7.9$ Hz, 1H), 6.66 (d, $^3J=9.5$ Hz, 1H), 2.53 ppm (s, 3H).

2-Bromo-quinolin-8-yl acetate (4):[26] 2-Oxo-1,2-dihydroquinolin-8-yl acetate (**3**; 300 mg, 1.47 mmol) and phosphoryltribromide (1.18 g, 4.1 mmol, 2.8 equiv) were refluxed in chloroform (1 mL; dried onto alumina) for 2 h under argon. At room temperature, the brown suspension was poured into ice, filtered, and washed with chloroform (30 mL). The organic layer was isolated and washed with brine (10 mL), dried (Na_2SO_4), filtered, and concentrated in vacuo. The brown oil was taken up in chloroform, treated with charcoal, and filtered through celite. The white crystals that appeared upon addition of a mixture of hexane and ethyl acetate (~1:1) were filtered to afford the expected bromide (137 mg, 35 %). ^{1}H NMR ($CDCl_3$): $\delta=8.00$ (d, $^3J=8.6$ Hz, 1H), 7.70 (dd, $^3J=8.0$ Hz, $^4J=1.5$ Hz,

 © 2005 Wiley-VCH Verlag GmbH & Co. KGaA, Weinheim

1H), 7.56 (t, $^3J=8.0$ Hz, 1H), 7.54 (d, $^3J=8.3$ Hz, 1H), 7.46 (dd, $^3J=7.5$ Hz, $^4J=1.5$ Hz, 1H), 2.50 ppm (s, 3H).

2-[2-(4-*n*-Butylphenyl)-6-(6-methylpyridin-2-yl)-pyrimidin-4-yl-quinolin-8-yl acetate (5): 2-Bromoquinolin-8-yl acetate (**4**; 306 mg, 1.15 mmol) was refluxed with 1,1,1,2,2,2-hexamethyldistannane (0.46 g, 1.4 mmol, 1.3 equiv) and tetrakistriphenylphosphinepalladium(0) (75 mg, 6.5×10^{-4} mol, 0.05 equiv) in distilled toluene (23 mL) under argon for 1.5 h. After removal of the solvent, the mixture was solubilized in fresh toluene (15 mL), and 2-(4-*n*-butylphenyl)-4-chloro-6-(6-methylpyridin-2-yl)pyrimidine (**2**; 423 mg, 1.26 mmol, 1.09 equiv) was added, together with tetrakistriphenylphosphinepalladium(0) (78 mg, 6.7×10^{-4} mol, 0.06 equiv). The solution was refluxed under argon for 17.5 h, after which the solvent was evaporated under vacuum. The residue was solubilized in chloroform (45 mL) and washed successively with water (15 mL) and brine (15 mL). The aqueous layer was extracted with chloroform (3×10 mL), and the combined organic layers were dried (Na_2SO_4), filtered, and concentrated in vacuo. A shiny white product (372 mg; 66%) was obtained after column chromatography (SiO_2, CH_2Cl_2/hexane 2.0:0.5) and recrystallization (CH_2Cl_2/EtOH). ^{1}H NMR ($CDCl_3$): $\delta=9.53$ (s, 1H), 8.91 (d, $^3J=8.5$ Hz, 1H), 8.66 (d, $^3J=8.2$ Hz, 2H), 8.57 (d, $^3J=7.9$ Hz, 1H), 8.39 (d, $^3J=8.8$ Hz, 1H), 7.80 (t, $^3J=7.6$ Hz, 1H), 7.81 (dd, $^3J=8.1$ Hz, $^4J=1.7$ Hz, 1H), 7.60 (t, $^3J=7.8$ Hz, 1H), 7.51 (dd, $^3J=7.5$ Hz, $^4J=1.7$ Hz, 1H), 7.38 (d, $^3J=8.2$ Hz, 2H), 7.29 (d, $^3J=7.6$ Hz, 1H), 2.81 (s, 3H), 2.74 (t, $^3J=7.8$ Hz, 2H), 2.68 (s, 3H), 1.70 (quint., $^3J=7.8$ Hz, 2H), 1.44 (sext., $^3J=7.5$ Hz, 2H), 0.97 ppm (t, $^3J=7.2$ Hz, 3H); ^{13}C NMR ($CDCl_3$): $\delta=170.0$, 164.2, 163.5, 158.1, 154.3, 154.0, 148.4, 145.8, 140.5, 137.0, 137.0, 135.5, 130.2, 128.6, 128.4, 127.1, 125.5, 124.8, 121.4, 119.5, 118.8, 111.5, 35.6, 33.5, 24.5, 22.4, 21.1, 14.0 ppm; R_f (SiO_2, CH_2Cl_2)$=0.31$; m.p. 209°C; FAB+: *m/z*: 489.2 ($[M\mathrm{H}]^+$), 446.2 ($[M-\mathrm{AcH}]^+$); elemental analysis calcd (%) for $C_{31}H_{28}N_4O_2\cdot0.08\,CH_2Cl_2$: C 75.36, H 5.73, N 11.32, O 6.46; found: C 75.38, H 5.55, N 11.40.

2-[2-(4-*n*-Butylphenyl)-6-(6-methylpyridin-2-yl)-pyrimidin-4-yl-quinolin-8-ol (LH):[27] A solution of 20% aqueous KOH (0.5 mL) was added to **5** (51 mg, 1.04 mmol) suspended in a mixture of pyridine (2 mL) and water (0.5 mL). The red solution was refluxed for 1 h and stirred at room temperature for another 10 h. After addition of CH_2Cl_2 (4 mL) and water (1 mL), the mixture was neutralized with dilute HCl and extracted with CH_2Cl_2 (2×4 mL). The combined organic layers were dried (Na_2SO_4), filtered, and concentrated in vacuo. After column chromatography (SiO_2, CH_2Cl_2 then CH_2Cl_2/EtOAc 2.0:0.3) and recrystallization from CH_2Cl_2/hexane, the desired alcohol (35 mg) was isolated in 76% yield. ^{1}H NMR ($CDCl_3$): $\delta=9.32$ (s, 1H), 8.84 (d, $^3J=8.5$ Hz, 1H), 8.63 (d, $^3J=8.2$ Hz, 2H), 8.53 (d, $^3J=7.9$ Hz, 1H), 8.46 (br s), 8.34 (d, $^3J=8.5$ Hz, 1H), 7.79 (t, $^3J=7.8$ Hz, 1H), 7.52 (t, $^3J=7.8$ Hz, 1H), 7.40 (dd, $^3J=7$ Hz, 1H), 7.37 (d, $^3J=8.2$ Hz, 2H), 7.29 (d, $^3J=8$ Hz, 1H), 2.73 (s, 3H), 2.73 (t, $^3J=7.8$ Hz, 2H), 1.70 (quint., $^3J=7.8$ Hz, 2H), 1.39 (sext., $^3J=7.5$ Hz, 2H), 0.98 ppm (t, $^3J=7.2$ Hz, 3H); ^{13}C NMR ($CDCl_3$): $\delta=164.5$, 164.3, 158.5, 154.1, 152.8, 152.7, 146.0, 137.9, 137.2, 137.1, 135.4, 129.3, 128.8, 128.7, 128.4, 125.0, 120.0, 119.1, 117.9, 111.3, 110.4, 35.7, 33.6, 24.7, 22.4, 14.0 ppm; R_f (SiO_2, CH_2Cl_2/EtOAc 2.0:0.3)$=0.25$; m.p. 165°C; EI: *m/z*: 446.3 ($[M]^-$); elemental analysis calcd (%) for $C_{31}H_{28}N_4O_2\cdot0.08\,CH_2Cl_2$: C 77.04, H 5.82, N 12.47, O 3.53; found: C 77.00, H 5.61, N 12.42.

Acknowledgements

A.P. acknowledges the support of the French Ministère de l'Éducation et de la Recherche by a predoctoral fellowship.

[1] a) *Molecular Switches* (Ed.: B. Feringa), Wiley-VCH, Weinheim, **2001**; b) A. P. de Silva, H. Q. N. Gunaratne, T. Gunnlaugsson, A. J. M. Huxley, C. P. McCoy, J. D. Rademacher, T. E. Rice, *Chem. Rev.* **1997**, *97*, 1515–1566.

[2] R. E. Stenkamp, D. C. Teller, K. Palczewski, *ChemBioChem* **2002**, *3*, 963–967.

[3] a) J.-M. Lehn, *Supramolecular Chemistry - Concepts and Perspectives*, **1995**, Ch. 8, 89–138; b) V. Balzani, A. Credi, M. Raymo, J. F. Stoddart, *Angew. Chem.* **2000**, *112*, 3484–4530; *Angew. Chem. Int. Ed.* **2000**, *39*, 3348–3391; c) J. F. Stoddart, *Acc. Chem. Res.* **2001**, *34*, 409–522.

[4] a) G. J. Brown, A. P. de Silva, S. Pagliari, *Chem. Commun.* **2002**, 2461–2462; b) A. P. de Silva, N. D. McClenaghan, *Chem. Eur. J.* **2004**, *10*, 574–586; c) F. M. Raymo, *Adv. Mater.* **2002**, *14*, 401–414; d) F. M. Raymo, S. Giordani, *Proc. Natl. Acad. Sci. USA* **2002**, *99*, 4941–4944.

[5] a) H. Tian, Y. Songjie, *Chem. Soc. Rev.* **2004**, *33*, 85–97; b) M. Irie, *Chem. Rev.* **2000**, *100*, 1685–1716; c) B. L. Feringa, R. A. van Delden, M. K. J. Ter Wiel, *Pure Appl. Chem.* **2003**, *75*, 563–575; d) V. Balzani, A. Credi, M. Venturi, *Pure Appl. Chem.* **2003**, *75*, 541–547; e) F. M. Raymo, M. Tomasulo, *Chem. Soc. Rev.* **2005**, *34*, 327–336.

[6] a) L. Fabbrizzi, M. Licchelli, P. Pallavicini, D. Sacchi, *Supramol. Chem.* **2001**, *13*, 569–582; b) J. H. R. Tucker, S. R. Collinson, *Chem. Soc. Rev.* **2002**, *31*, 147–156.

[7] a) L. Zelikovich, J. Libman, A. Shanzer, *Nature* **1995**, *374*, 790–792; b) C. Canevet, J. Libman, A. Shanzer, *Angew. Chem.* **1996**, *108*, 2842–2845; *Angew. Chem. Int. Ed. Engl.* **1996**, *35*, 2657–2660; c) C. Belle, J.-L. Louis, E. Saint-Aman, *New J. Chem.* **1998**, *22*, 1399–1402.

[8] J.-P. Collin, J.-M. Kern, L. Raehm, J.-P. Sauvage, *Molecular Switches* (Ed.: B. Feringa), Wiley-VCH, Weinheim, **2001**, 249–280.

[9] A. Petitjean, R. G. Khoury, N. Kyritsakas, J.-M. Lehn, *J. Am. Chem. Soc.* **2004**, *126*, 6637–6647.

[10] M. Barboiu, L. Prodi, M. Montali, N. Zaccheroni, N. Kyritsakas, J.-M. Lehn, *Chem. Eur. J.* **2004**, *10*, 2953–2959.

[11] A. Petitjean, N. Kyritsakas, J.-M. Lehn, *Chem. Commun.* **2004**, 1168–1169.

[12] K. Von Burdeska, H. Fuhrer, G. Kabas, A. E. Siegrist, *Helv. Chim. Acta* **1981**, *64*, 113–152.

[13] D. P. Funeriu, J.-M. Lehn, G. Baum, D. Fenske, *Chem. Eur. J.* **1997**, *3*, 99–104.

[14] *Organic Syntheses*, Collective volume III, (Ed.: R. L. Danheiser), Wiley, New York, **1981**, pp. 136–138.

[15] a) S. T. Howard, *J. Am. Chem. Soc.* **1996**, *118*, 10269–10274; b) A. Göller, U.-W. Grummt, *Chem. Phys. Lett.* **2000**, *321*, 399–405; c) G. Corongiu, P. Nava, *Int. J. Quantum Chem.* **2003**, *93*, 395–404.

[16] a) G. S. Hanan, J.-M. Lehn, N. Kyritsakas, J. Fischer, *J. Chem. Soc. Chem. Commun.* **1995**, 765–766; b) M. Okhita, J.-M. Lehn, G. Baum, D. Fenske, C *hem. Eur. J.* **1999**, *5*, 3471–3481; c) K. M. Gardinier, R. G. Khoury, J.-M. Lehn, *Chem. Eur. J.* **2000**, *6*, 4124–4131; d) J.-L. Schmitt, A.-M Stadler, N. Kyritsakas, J.-M. Lehn, *Helv. Chim. Acta* **2003**, *86*, 1598–1624.

[17] a) The variation of the chemical shifts of the proton signals was analyzed using the Chem. Equili. Software (version 6.1, 1998, V. P. Solov'ev, Moscow University); b) Binding constants based on UV/Vis titrations performed by Dr. Annie Marquis (private communication) and fitted with LETAGROP, consistent with the association constants reported for L=5,5′-dimethyl-2,2′-bipyridine ($K_{CuL}=6.0\pm0.3$, see: F. Arnaud-Neu, M. Sanchez, M.-J. Schwing-Weil, *Nouv. J. Chim.* **1986**, *10*, 165–167.

[18] P. J. Burke, D. R. McMillin, W. R. Robinson, *Inorg. Chem.* **1980**, *19*, 1211–1214.

[19] For examples of grids containing different metal ions or different coordination sites, see for instance: a) D. M. Bassani, J.-M. Lehn, K. Fromm, D. Fenske, *Angew. Chem.* **1998**, *110*, 2534–2537; *Angew. Chem. Int. Ed.* **1998**, *37*, 2364–2367; b) L. Uppadine, J.-M. Lehn, *Angew. Chem.* **2004**, *116*, 242–245; *Angew. Chem. Int. Ed.* **2004**, *43*, 240–243; c) L. Kovbasyuk, H. Pritzkow, R. Krämer, *Eur. J. Inorg. Chem.* **2005**, 894–900.

[20] J.-M. Lehn, *Supramolecular Chemistry - Concepts and Perspectives*, **1995**, pp. 139–160; J.-M. Lehn, *Chem. Eur. J.* **2000**, *6*, 2097–2102.

[21] For some recent references, see for instance: a) F. M. Raymo, S. Giordani, *J. Am. Chem. Soc.* **2001**, *123*, 4651–4652; b) A. P. de Silva, I. M. Dixon, H. Q. N. Gunaratne, T. Gunnlaugsson, P. R. S. Maxwell, T. E. Rice, *J. Am. Chem. Soc.* **1999**, *121*, 1393–1394; c) A. P. de Silva, N. D. McClenaghan, *J. Am. Chem. Soc.* **2000**, *122*, 3965–3966; d) A. Saghatelian, N. H. Völcker, K. M. Guckian, V. S.-Y. Lin, M. R.

 © 2005 Wiley-VCH Verlag GmbH & Co. KGaA, Weinheim

Ghadiri, *J. Am. Chem. Soc.* **2003**, *125*, 346–347; e) D. Margulies, G. Melman, C. E. Felder, R. Arad-Yellin, A. Shanzer, *J. Am. Chem. Soc.* **2004**, *126*, 15400–15401.

[22] a) For an example of multistate all optical switching device, see: G. M. Tsivgoulis, J.-M. Lehn, *Adv. Mater.* **1997**, *9*, 627–630; b) for an optical-protonic system, see: M. C. Moncada, A. J. Parola, C. Lodeiro, F. Pina, M. Maestri, V. Balzani, *Chem. Eur. J.* **2004**, *10*, 1519–1526; c) for logic operations in gene expression modulation, see: S. Istrail, E. H. Davidson, *Proc. Natl. Acad. Sci. USA* **2005**, *102*, 4954–4959.

[23] R. H. Wiley, S. C. Slaymaker, H. Kraus, *J. Org. Chem.* **1957**, *22*, 204–207.

[24] A. V. Rama Rao, S. P. Chavan, L. Sivadasan, *Tetrahedron* **1986**, *42*, 5065–5071.

[25] G. R. Pettit, W. C. Fleming, K. D. Paull, *J. Org. Chem.* **1968**, *33*, 1089–1092.

[26] H. Gershon, D. D. Clark, *Monatsh. Chem.* **1991**, *122*, 935-942.

[27] K. Mekouar, J.-F. Mouscadet, D. Desmaële, F. Subra, H. Leh, D. Savouré, C. Auclair, J. d′Angelo, *J. Med. Chem.* **1998**, *41*, 2846–2857.

Received: June 2, 2005
Published online: August 17, 2005

 © 2005 Wiley-VCH Verlag GmbH & Co. KGaA, Weinheim